J Electroceram (2014) 32:175–179
DOI 10.1007/s10832-013-9864-2

Low temperature sintering of $Ba_{0.91}Ca_{0.09}Ti_{0.916}Sn_{0.084}O_3$ lead-free piezoelectric ceramics with the additives of ZnO and MnO_2

Qiang Chen · Tao Wang · Jiagang Wu · Xiaojing Cheng · Xiaopeng Wang · Binyu Zhang · Dingquan Xiao · Jianguo Zhu

Received: 26 May 2013 / Accepted: 8 September 2013 / Published online: 28 September 2013

Abstract The objective of this work is to lower the sintering temperature of $Ba_{0.91}Ca_{0.09}Ti_{0.916}Sn_{0.084}O_3$ (BCTS) ceramics without sacrificing the piezoelectric performance. The low-temperature sintering technique has been conducted to prepare the BCTS ceramics by adding two additives of ZnO and MnO_2. The ceramics endure a phase transition from a ferroelectric tetragonal phase to a pseudo-cubic relaxor ferroelectric with increasing MnO_2 content. The addition of ZnO and MnO_2 decreases the sintering temperature greatly, positively affecting their dielectric and piezoelectric properties. An enhanced electrical behavior of d_{33} ~495 pC/N, k_p ~43.0 %, ε_r ~5429, and tan δ ~1.54 % has been observed in the ceramic with x = 0.1 wt% when sintered at ~1315 °C. As a result, the method to dope two additives of ZnO and MnO_2 can effectively improve the piezoelectric properties of $BaTiO_3$-based ceramics sintered at a low temperature.

Keywords Lead-free ceramic · $Ba_{0.91}Ca_{0.09}Ti_{0.916}Sn_{0.084}O_3$ · Low temperature sintering · Piezoelectricity

1 Introduction

In 2011, a giant piezoelectric constant (d_{33}~510~568 pC/N) of $BaTiO_3$ ceramics has been obtained using Ca and Sn substitutions for the Ba and Ti sites, while a high sintering temperature of >1450 °C can only warrant obtaining such a high d_{33} [1–3]. However, such a high processing temperature easily results in a poor stability of electrical properties due to their compositional changes, and a low temperature sintering method can satisfy the demand for cofiring piezoelectric ceramics with metal electrodes for device applications. As a result, it is highly desirable to lower the sintering temperature of such a ceramic without sacrificing their electrical properties. In addition, the low sintering temperature reduces the energy consumption, decreases the fabrication cost, and improves the reproducibility.

Some efforts have been conducted to lower the sintering temperature of $BaTiO_3$-based piezoelectric ceramics [4–7], and the liquid-phase sintering is a very effective tool to reduce its processing temperature greatly [4–7]. The introduction of additives makes piezoelectric ceramics denser at a low processing temperature by the formation of a liquid phase, promoting the densification process by rearranging particles and promoting material transport [8–13]. For a low temperature sintering of Ca and Zr or Ca and Sn -modified $BaTiO_3$ ceramics, some additives have been widely used [4–7], such as, La_2O_3 [4], Bi_2O_3 [5], MnO [6], and $BiFeO_3$ [7]. However, their sintering temperature and piezoelectric properties can be simultaneously reduced by the introduction of these additives [4–7], or their sintering temperature can be very slowly decreased for maintaining a high d_{33} [14]. Recently, it has been found that one more additives more benefit the improvement in the microstructure and electrical properties of piezoelectric materials. For example, doping MnO_2 and CuO is an effective way to promote the densification and electrical properties of $K_xNa_{1-x}NbO_3$ ceramics [15], and an enhanced piezoelectric behavior has also been observed in the MnO_2 and CuO -modified $0.95(Na_{0.5}K_{0.5})NbO_3$-$0.05BaTiO_3$ ceramics when sintered at a low temperature of 950 °C [16]. A high d_{33} of ~521 pC/N has been observed for the ZnO -modified

Q. Chen · T. Wang · J. Wu (✉) · X. Cheng · X. Wang · B. Zhang · D. Xiao · J. Zhu
Department of Materials Science, Sichuan University, Chengdu 610064, People's Republic of China
e-mail: msewuj@scu.edu.cn

J. Wu
e-mail: wujiagang0208@163.com

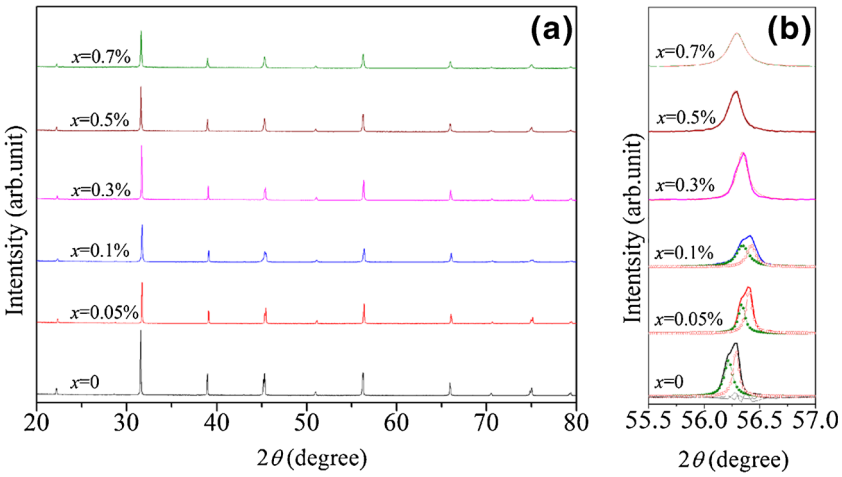

Fig. 1 (**a**) XRD patterns and (**b**) expanded XRD patterns of BCTS-0.1wt%ZnO-xMnO$_2$ ceramics, where these peaks located at 55.5~57.0° were fitted by the Lorentz method

$Ba_{0.85}Ca_{0.15}Ti_{0.90}Zr_{0.10}O_3$ ceramics by us, while a relatively high sintering temperature of 1450 °C is necessary [14]. As a result, this objective of this work is to reduce the sintering temperature of Ca and Sn -modified $BaTiO_3$ ceramics without decreasing its d_{33} using the additives of ZnO and MnO_2.

In this work, the $Ba_{0.91}Ca_{0.09}Ti_{0.916}Sn_{0.084}O_3$ lead-free piezoelectric ceramics are sintered by introducing two additives of MnO_2 and ZnO. Their sintering temperature decreases dramatically, while a large d_{33} of~495 pC/N has been obtained. Some related physical mechanisms have been addressed.

2 Experimental procedure

$(Ba_{0.91}Ca_{0.09}Ti_{0.916}Sn_{0.084}O_3+0.1wt\%ZnO)+x\,wt\%MnO_2$ (BCTS-0.1wt%ZnO-xMnO$_2$, x~0~0.7 wt%) lead-free piezoelectric ceramics were prepared by the conventional solid-state method using these raw materials of $BaCO_3$ (99 %, Sinopharm Chemical Reagent Co., Ltd, China), $CaCO_3$ (99 %, Sinopharm Chemical Reagent Co., Ltd, China), TiO_2 (98 %, Sinopharm Chemical Reagent Co., Ltd, China), SnO_2 (99 %, Sinopharm Chemical Reagent Co., Ltd, China), ZnO (99 %, Sinopharm Chemical Reagent Co., Ltd, China), and MnO_2 (99 %, Sinopharm Chemical Reagent Co., Ltd, China). These powders are weighed according to the stoichiometric ratio of BCTS-0.1wt%ZnO ceramics, are ball-milled in ethanol using zirconia balls for 24 h, dried, and then calcined at 1200 °C for 3 h. The MnO_2 with different content (x=0.05, 0.1, 0.3, 0.5, and 0.7 wt%) was added to BCTS-0.1wt%ZnO after calcination. This mixture is re-milled for 24 h, dried, and then re-calcined at 1200 °C for 3 h. These sintered powders are mixed using a PVA binder solution, pressing into the disk sample with a diameter of 1.0 cm and a thickness of 1.0 mm. These disk samples are sintered at a temperature range of 1275~1380 °C for 3 h in

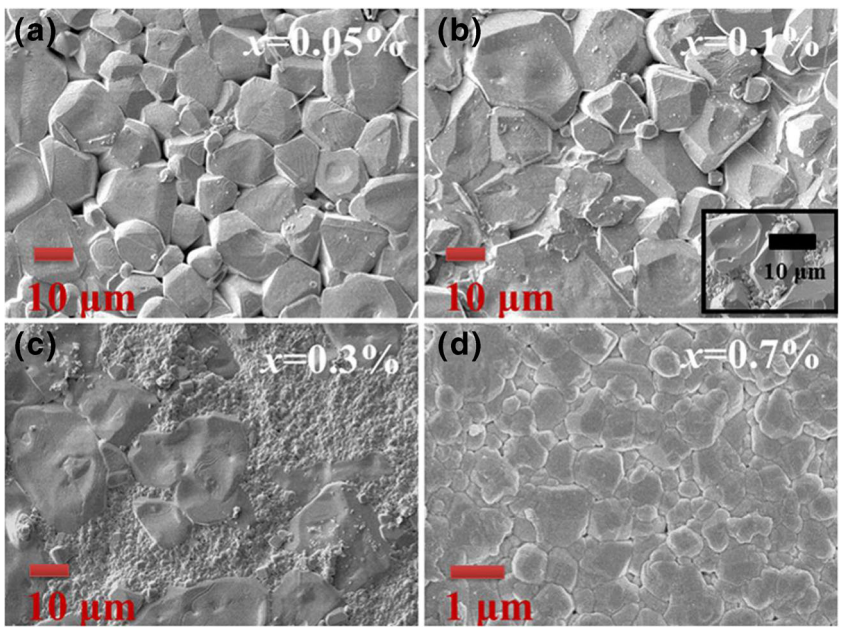

Fig. 2 SEM morphologies of BCTS-0.1wt%ZnO-xMnO$_2$ ceramics (**a**) x=0.05 wt%, (**b**) x=0.1 wt%, (**c**) x=0.3 wt%, and (**d**) x=0.7 wt%, the inset in (**b**) is expanded SEM pattern

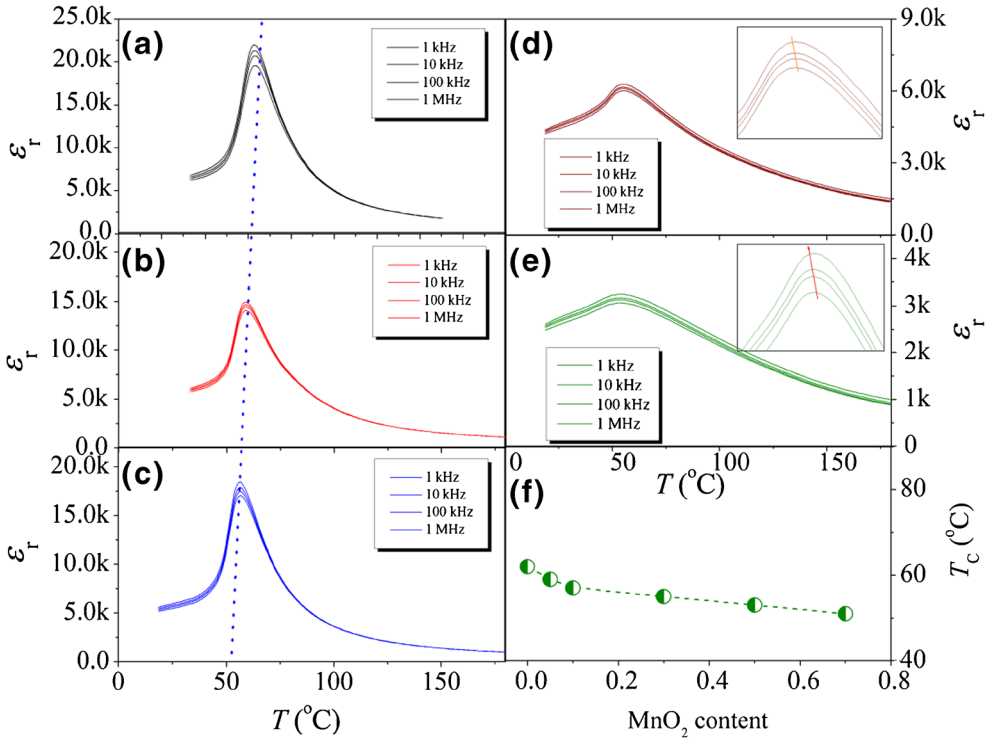

Fig. 3 Temperature dependence of the dielectric constant of BCTS-0.1wt%ZnO-xMnO$_2$ ceramics (**a**) x=0 wt %, (**b**) x=0.05 wt %, (**c**) x=0.1 wt%, (**d**) x=0.3 wt %, (**e**) x=0.5 wt %, and (**f**) the composition dependence of T_c

air, and were coated with silver paste to form electrodes on both sides and fired at 700 °C for 10 min. A *dc* field of 4 kV/mm at a temperature of 40 °C has been used to pole these ceramics under a silicone oil bath

The phase structure of the sintered ceramics was measured by X-ray diffraction (XRD) analysis (Bruker D8 Advanced XRD, Bruker AXS Inc., Madison, WI, CuKa). Scanning electron microscopy has been used to characterize the surface morphologies of these sintered ceramics (JSM 5900, Japan). The capacitance and dissipation factors of the sintered samples were measured using an *LCR* analyzer (HP 4980, Agilent, U.S.A.) with a varied temperature between room temperature~180 °C. Their dielectric constant and loss tangent were measured by a *LCR* meter (HP 4294, USA), and their piezoelectric constant (d_{33}) was measured using a piezo-d_{33} meter (ZJ-6A, China). *P-E* hysteresis loops of these ceramics were measured using a Radiant Precision Workstation (USA) at 10 Hz.

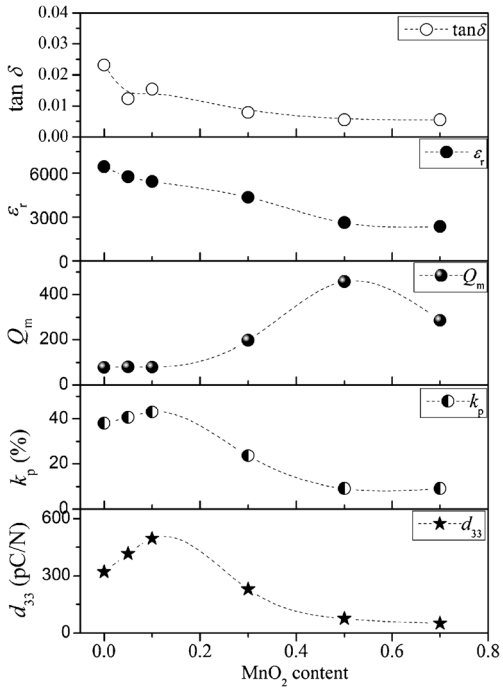

Fig. 4 d_{33}, k_p, ε_r, tan δ, and Q_m of BCTS-0.1wt%ZnO-xMnO$_2$ ceramics

3 Results and discussion

The XRD patterns of BCTS-0.1wt%ZnO-xMnO$_2$ ceramics were characterized for studying the effect of these sintered aids on their phase structure, as shown in Fig. 1(a). All the ceramics

Table 1 Sintering temperature and electrical properties of BCTS-0.1wt%ZnO -xMnO$_2$ ceramics

x wt%	T_S (°C)	d_{33} (pC/N)	k_p	Q_m	tan δ (%) (100 kHz)	ε_r (100 kHz)
x=0	1380	320	0.38	78	2.31 %	6440
x=0.05	1335	415	0.41	80	1.24 %	5758
x=0.1	1315	495	0.43	80	1.54 %	5429
x=0.3	1290	228	0.24	197	0.79 %	4342
x=0.5	1280	75	0.09	458	0.55 %	2621
x=0.7	1275	50	0.09	286	0.54 %	2353

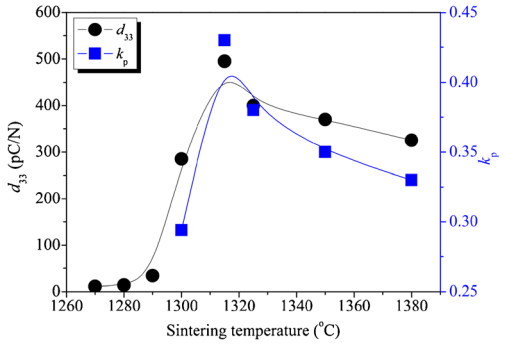

Fig. 5 Sintering temperature -dependent piezoelectric properties of BCTS-0.1wt%ZnO-0.1wt%MnO_2 ceramics

have a pure perovskite structure without any secondary phases, showing the formation of a stable solution. To further investigate their phase structure, the expanded XRD patterns of MnO_2 -modified BCTS-0.1wt%ZnO ceramics were shown in Fig. 1(b). These diffraction peaks shift to a high angle initially due to the smaller ionic radius of the Mn^{4+} substitution for Ti^{4+} and Sn^{4+}, and subsequently the peaks position is shifted to a low angle with an increase in MnO_2 contents (x>0.3 wt%) because the excessive MnO_2 locates at the grain boundaries and the Zn^{2+} substitutes for (Ti, Sn)$^{4+}$. Similar phenomenon has been observed in the CuO and MnO_2 -doped 0.92($K_{0.48}Na_{0.54}$)NbO_3-0.08$LiNbO_3$ [17]. Moreover, these peaks are splitted at x<0.3 wt%, showing a tetragonal phase. A single peak is observed at x≥0.3 wt% with increasing x (x>0.3 wt%), showing the involvement of a pseudocubic phase in these ceramics. As a result, the introduction of MnO_2 results in the change of the phase structure of BCTS-0.1wt%ZnO ceramics.

To clearly study the MnO_2 effect on the surface morphologies of BCTS-0.1wt%ZnO ceramics, the SEM patterns are shown in Fig. 2(a)–(d). Their grain size becomes larger with increasing x (x≤0.1 wt%), the ceramic with x=0.3 wt% has a bimodal grain size distribution, and then are refined with further increasing x. Comparing Fig. 2(b) with Fig. 2(d), the grain size of the ceramic with x=0.1 wt% is ten times as large as that of the one with x=0.7 wt%. The underlying physical mechanisms have been reasonably explained below: a low content of MnO_2 promotes the grain growth of BCTS-0.1wt%ZnO ceramics by entering the lattice, while the excessive MnO_2 clusters their grain boundaries, prohibiting the grain growth. As a result, the increase in the grain size could benefit the improvement in the piezoelectric constant (d_{33}) of BCTS-0.1wt%ZnO-$x$$MnO_2$ ceramics.

The temperature dependence of the dielectric constant (ε_r) of BCTS-0.1wt%ZnO-$x$$MnO_2$ ceramics is measured at 1 kHz ~1 MHz, as shown in Fig. 3(a)–(e). As shown in Fig. 3(a)–(e), all the ceramics have only one phase transition (T_C), showing an involvement of a tetragonal phase at x<0.3 wt%, as shown in Fig. 1. The T_C peaks become gradually broadened in the range of x>0.1 wt%, and similar phenomena have been observed in other piezoelectric materials because of a small grain size [18, 19]. Moreover, the inset in Fig. 3(d) and (e) shows that excessive MnO_2 also results in the relaxor behavior of these ceramics [20–26]. Figure 3(f) plots their T_C values as a function of x. Their T_C values slightly lower with increasing MnO_2 content (x~0~0.7 wt%), showing that adding a higher MnO_2 content causes the decrease of the T_C.

Subsequently, the effect of MnO_2 content on the dielectric and piezoelectric properties of BCTS-0.1wt%ZnO ceramics is studied, as plotted in Fig. 4. The ε_r gradually decreases, and the dielectric loss (tan δ) almost drops with increasing x. It is of great note to that the mechanical quality factor (Q_m) increases

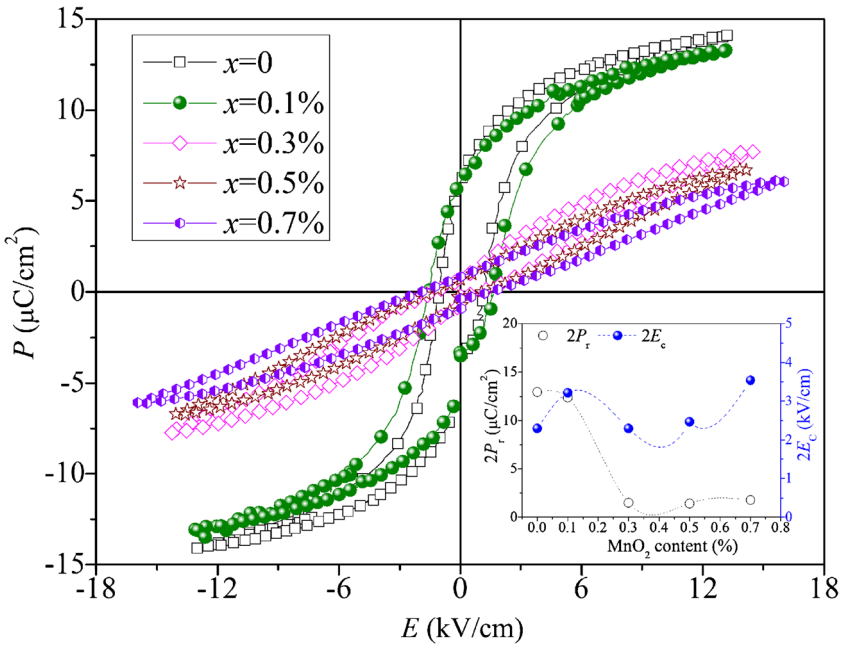

Fig. 6 *P-E* loops of BCTS-0.1wt%ZnO-$x$$MnO_2$ ceramics, and the inset is $2P_r$ and $2E_c$ values as a function of MnO_2 content

and slightly decreases for $x>0.5$ wt% because the MnO_2 as an additive causes the "hardening" effects. The d_{33} increases with increasing x and then decreases, reaching a maximum value of 495 pC/N at $x=0.1$ wt%. Similarity to the change of the d_{33}, the k_p also gets a maximum value of 0.43 at $x=0.1$ wt%. As a result, maximum d_{33} and k_p values are observed in the ceramic with $x=0.1$ wt%, as shown in Fig. 4 and Table 1. In this work, the dramatic decrease in piezoelectric properties of the ceramics with $x>0.3$ wt% MnO_2 could be attributed to the involvement of a phase transition from a ferroelectric tetragonal phase to a pseudo-cubic relaxor ferroelectric with increasing MnO_2 content [20–26]. Figure 5 shows the sintering temperature dependence of the piezoelectric properties of BCTS-0.1wt%ZnO-$x$$MnO_2$ ceramics. In this work, the piezoelectric properties strongly depend on the sintering temperature. The d_{33} almost disappears when the sintering temperature is below 1290 °C, and a higher sintering temperature also leads to the decrease of d_{33}. Therefore, an optimum sintering temperature of 1315 °C enhances the piezoelectric properties of this work. Similar result has been observed in the BCTZ ceramics [27]. Till now, there are few reports on such a large d_{33} of BCTS ceramics when sintered at such a low temperature of ~1315 °C. As a result, an enhanced d_{33} value could be attributed to the introduction of the optimum ZnO and MnO_2 content of this work.

Figure 6 plots the *P-E* loops of BCTS-0.1wt%ZnO-$x$$MnO_2$ ceramics with different MnO_2 content, measured at 10 Hz and room temperature. A typical *P-E* loop has been demonstrated in the ceramics with $x<0.3$ wt%, while these ceramics with $x\geq 0.3$ wt% have a slim *P-E* loop. The inset in Fig. 6 plots their $2P_r$ and $2E_c$ values as a function of MnO_2 content. The $2P_r$ slowly decreases at $x<0.3$ wt% and drops dramatically with further increasing MnO_2 content owing to the involvement of the relaxor behavior [20–26], while there is no significant difference for these ceramics with increasing the content ($x\geq 0.3$ wt%). In addition, the $2E_c$ is in the range of 2.3~3.6 kV/cm.

4 Conclusions

$Ba_{0.91}Ca_{0.09}Ti_{0.916}Sn_{0.084}O_3$ lead-free piezoelectric ceramics were prepared at a low sintering temperature by adding two additives of ZnO and MnO_2. The addition of ZnO and MnO_2 effectively decreases the sintering temperature, resulting in an improvement in their dielectric and piezoelectric properties. Such a ceramic with $x=0.1$ wt% has an enhanced electrical behavior of d_{33}~495 pC/N, k_p~43.0 %, ε_r~5429, and tan δ~1.54 % when sintered at a low temperature of ~1315 °C. As a result, such a method provides a useful reference to the low-temperature sintering $BaTiO_3$-based piezoelectric ceramics

Acknowledgments Authors gratefully acknowledge the supports of the National Science Foundation of China (NSFC Nos. 51102173 and 51272164), the introduction of talent start funds of Sichuan University (2082204144033), and the Fundamental Research Funds for the Central Universities (2012SCU04A01).

References

1. D. Xue, Y. Zhou, H. Bao, J. Gao, C. Zhou, X. Ren, Appl. Phys. Lett. **99**, 122901 (2011)
2. W. Li, Z. Xu, R. Chu, P. Fu, G. Zang, J. Am. Ceram. Soc. **94**(12), 4131 (2011)
3. L.F. Zhu, B.P. Zhang, X.K. Zhao, L. Zhao, P.F. Zhou, J.F. Li, J. Am. Ceram. Soc. **96**(1), 241 (2013)
4. Q. Lin, M. Jiang, D.M. Lin, Q.J. Zheng, X.C. Wu, X.M. Fan, J. Am. Ceram. Soc. **24**(2), 734 (2013)
5. T. Chen, T. Zhang, J.F. Zhou, J.W. Zhang, Y.H. Liu, G.C. Wang, Mater. Res. Bull. **47**(4), 1104 (2012)
6. J. Wu, Z. Wang, B. Zhang, J.G. Zhu, D.Q. Xiao, Integr. Ferroelectr. **141**, 89 (2013)
7. J.G. Wu, W.J. Wu, D.Q. Xiao, J. Wang, Z.C. Yang, Z.H. Peng, Q. Chen, J.G. Zhu, Curr. Appl. Phys. **12**(2), 534 (2012)
8. K. Wang, J.F. Li, N. Liu, Appl. Phys. Lett. **93**(9), 092904 (2008)
9. C.W. Ahn, H.C. Song, S. Nahm, S. Priya, J. Am. Ceram. Soc. **89**(3), 921 (2006)
10. S.M. Lee, S.H. Lee, C.B. Yoon, H.E. Kim, K.W. Lee, J. Electroceram. **18**, 311 (2007)
11. H. Park, C. Nam, I. Seo, J. Choi, S. Nahm, J. Am. Ceram. Soc. **93**(9), 2537 (2010)
12. J. Yoo, S. Lee, J. Electroceram. **23**, 432 (2009)
13. T. Lee, S. Lee, J. Yeo, D. Kim, J. Electroceram. **30**, 213 (2013)
14. J. Wu, D. Xiao, W. Wu, Q. Chen, J. Zhu, Z. Yang, J. Wang, Scripta Mater. **65**(9), 771 (2011)
15. D. Lin, K.W. Kwok, H.L.W. Chan, J. Alloys Compd. **461**, 273 (2008)
16. C.W. Ahn, S. Nahm, M. Karmarkar, D. Viehland, D.H. Kang, K.S. Bae, S. Priya, Mater. Lett. **62**, 3594 (2008)
17. Q. Yin, S. Yuan, Q. Dong, C. Tian, J. Alloys Compd. **491**(1–2), 340 (2010)
18. Y. Park, W.J. Lee, H.G. Kim, J. Phys. Condens. Matter **9**, 9445 (1997)
19. S. Chattopadhyay, P. Ayyub, V.R. Palkar, M. Multani, Phys. Rev. B **52**, 13177 (1995)
20. V.V. Shvartsman, D.C. Lupascu, J. Am. Ceram. Soc. **95**(1), 1 (2012)
21. V.V. Shvartsman, J. Dec, Z.K. Xu, J. Banys, P. Keburis, W. Kleemann, Phase Transit. **81**, 1013 (2008)
22. V.V. Shvartsman, J. Zhai, W. Kleemann, Ferroelectrics **379**, 77 (2009)
23. V.V. Shvartsman, W. Kleemann, J. Dec, Z.K. Xu, S.G. Lu, J. Appl. Phys. **99**, 124111 (2006)
24. V.V. Shvartsman, M.E.V. Costa, M. Avdeev, A.L. Kholkin, Ferroelectrics **296**, 187 (2003)
25. V.V. Shvartsman, A.L. Kholkin, A. Orlova, D. Kiselev, A.A. Bogomolov, A. Sternberg, Appl. Phys. Lett. **86**, 202907 (2005)
26. D.C. Lupascu, T. Granzow, T. Woike, Europhys. Lett. **68**, 733 (2004)
27. J. Wu, D. Xiao, B. Wu, W. Wu, J. Zhu, Z. Yang, J. Wang, Mater. Res. Bull. **47**, 1281 (2012)